

WAKEFIELD EFFECTS EVALUATION ON NANOMETER SMALL BEAM AT KEK-ATF

Y. Abe*, SOKENDAI, Tsukuba, Japan

K. Kubo, T. Okugi, N. Terunuma, KEK and SOKENDAI, Tsukuba, Japan

Abstract

The KEK Accelerator Test Facility (ATF) is an R&D facility for the final focus system to develop the nanometer beam technology required for the International Linear Collider. We have confirmed 41 nm vertical beam size at the focal point of the KEK-ATF final focus test beamline, while the original designed goal is 37 nm. However, strong intensity dependence of the beam size exists due to wakefield. In order to produce the small beam stably, clear understanding of wakefield effects is necessary. In past studies, simulation results were compared with experiments and showed that the influence of some vacuum components and BPMs were significant. However, these results did not well agree quantitatively. Further investigations of the wakefield effect to the beam are being performed with more realistic simulations of the wakefield calculation including some wakefield sources, which were not considered in the past studies. This report presents the current status of the research.

INTRODUCTION

The Accelerator Test Facility (ATF) at KEK is a R&D facility for beam control and measurement techniques to develop nanometer level beam required for the International Linear Collider (ILC) [1]. The goal is to realize 37-nm vertical beam size and develop beam position control technology in the nanometer level (ATF2 project). The facility consists of an injector, a LINAC, a Damping Ring, and an extraction (EXT) and a final focus (FF) beamline (ATF2 beamline shown in Fig. 1). In 2016, it was confirmed that the beam size reached 41 nm. The beam size at ATF depends on the bunch intensity mainly due to wakefield. In November 2016, the ATF2 beamline was substantially modified to investigate the effect of wakefield. The intensity dependence was mitigated after removal of some wakefield sources and modification of some vacuum components from the FF beamline. Understanding the effects of wakefield is important for realizing stable nanometer beam [2].

The simulation results were compared with experimental results and shown that some vacuum components and BPMs had significant effect [3–5]. However, the experimental results were twice as large as the simulation results [5]. We suspect some non-negligible wakefield sources exist which had not been included in the simulations. Our past analysis considered only the major wake sources (bellows, cavity BPM and vacuum flanges). Therefore, we performed simulations reproducing more realistic beamlines to confirm more detailed effects on the beam. We considered some vacuum components located in EXT line and shielded components in

FF line, and their misalignment and deformation. This paper reports updated wakefield calculations and their effects on the beams.

WAKEFIELD CALCULATION

A wakefield is an excited electromagnetic field generated by a beam passing through a structure. A particle at a longitudinal position s_w with respect to the bunch center will be kicked by $\Delta p_{x,y}$, expressed as $q_1 W_{x,y}(x, y, s_w)$ where the transverse wakepotential is defined as:

$$W_{x,y}(x, y, s_w) \equiv \frac{e}{q_1} \int \{E_z(x, y, z, t) \mp cB_{y,x}(x, y, z, t)\} dz, \quad (1)$$

where we assume an ultra-relativistic beam passing transverse position x and y , the bunch center passes $z = 0$ at time $t = 0$, q_1 is the total bunch charge, and $t = (z + s_w)/c$.

The excited wakefield is calculated by GdfidL [6] which is an electromagnetic field simulation code. Wakefield sources at ATF2 beamline is shown in Fig. 1. The 3D models were constructed to reproduce the actual geometrical shape of the wakefield sources. For example, a model of 5-mm deforming bellows with RF shield is shown in Fig. 2. We assumed that a normal distribution bunch with root mean square (RMS) length of 7.0 mm. Figure 3 shows the calculated wake potentials. The vertical axis shows the wake potential of the beam passing $y = 1$ mm offset from the geometrical center, and the horizontal axis shows the distance from the beam center s_w . Table 1 shows the peak of the wakepotential, quantity and location of wakefield sources.

We evaluated the beam size by using the position of simulated particles at virtual interaction point (IP), where the beam size is minimized at ATF2 beamline, to evaluate the effects on small beam. The position change of the particle at the IP, Δy_{IP} , is calculated approximately as Eq. 2, where i is the index for all wakefield sources, a_i is the vertical misalignment of the source, β_i the beta-function at the source, β_{IP} the beta-function at IP, and $\Delta \phi_i$ is the phase advance from the source to IP [8]:

$$\Delta y_{IP} \approx \frac{q_1}{E} W_y(x = 0, a_i, s_w) \sqrt{\beta_{\text{wake}} \beta_{IP}} \sin \Delta \phi_i. \quad (2)$$

The wakefield effect of each type of source can be expressed by $W_{s\text{-eff}}$, from the RMS of Eq. 2, considering many beamlines with different sets of random misalignments with RMS a in a unit of mm, as:

$$\begin{aligned} (\text{RMS of } \Delta y_{IP}) &\approx \frac{q_1}{E} \sqrt{\beta_{IP}} W_{s\text{-eff}} \\ W_{s\text{-eff}} &\equiv a W_y(0, 1) \sum_i \sqrt{\beta_i} \sin \Delta \phi_i \end{aligned} \quad (3)$$

* abeyuki@post.kek.jp

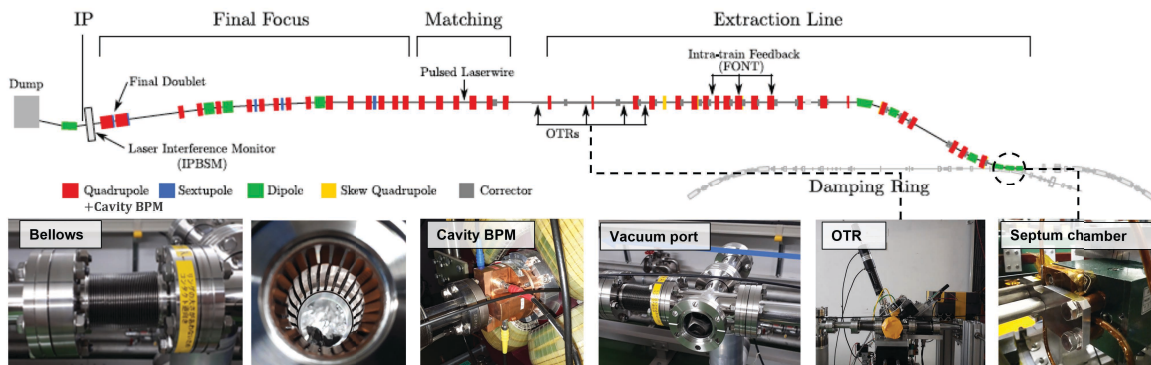


Figure 1: ATF2 beamline layout and wakefield sources.

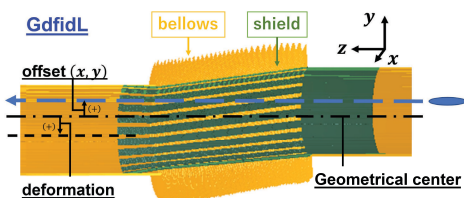


Figure 2: GdfidL calculated model of deformed bellows with wakefield mitigation shield.

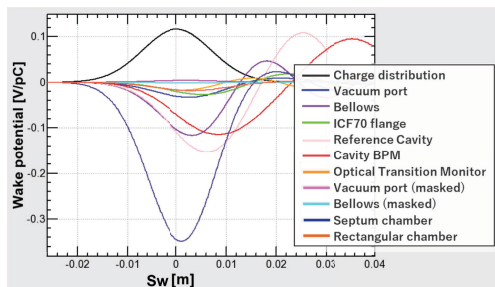


Figure 3: Transverse wakepotentials in ATF2 beamline by GdfidL. Vertical: wake potential $W_y(0, 1)$, horizontal: distance from bunch center s .

where, an approximation is used, replacing s_W -depending $W_{y,i}(x=0, y=1 \text{ mm}, s_w)$ by its peak $W_y(0, 1) \equiv \max[|W_{y,i}(x=0, y=1 \text{ mm}, s_w)|]$. The effects of the wakefield is related to the quantity and β function at wakefield sources. For example, septum magnet chamber has four times stronger wake potential than cavity BPM. However, estimated effect $W_{s\text{-eff}}$ is weaker than cavity BPM. The detail effects of the wakefield are discussed in the next section. We also calculated deformed bellows, which have not been considered in the past studies. The results are shown in Fig. 4, where the vertical axis shows the peak of the wake potential for different deformations from 1 to 5 mm as in Fig. 2. Lines show 3rd order polynomial fittings. The excited wakefield is mitigated to around 1/10 by the shield.

TRACKING SIMULATION

The effects of short range wakefield on the bunch were evaluated by Strategic Accelerator Design (SAD) [7] which

MC5: Beam Dynamics and EM Fields

D01: Beam Optics - Lattices, Correction Schemes, Transport

Table 1: Peak Wakepotential at Beam Offset $y = 1 \text{ mm}$, Random Misalignment RMS $a = 1 \text{ mm}$.

	Wakefield source	Qty	$W_y(0, 1)$	$W_{s\text{-eff}}$
EXT	Bellows	51	0.117	4.07
	Septum magnet chamber*	3	0.440	0.54
	Vacuum port	15	0.027	0.59
	Optical Transition Radiation monitor	4	0.021	0.03
FF	Cavity BPM	24	0.115	10.10
	Shielded bellows*	37	0.001	0.44
	Shielded vac. port*	14	0.004	0.45
EXT	Vacuum Flange (ICF70)	112	0.028	2.52
FF	Reference Cavity	2	0.154	2.18

EXT: EXTRAction beamline, FF: Final Focus beamline

*newly calculated

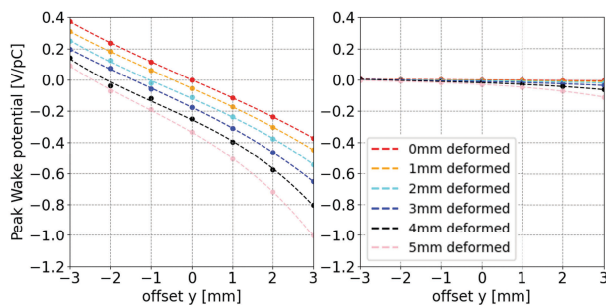


Figure 4: Transverse peak wakepotentials of deformed bellows. Left: bellows without shield, Right: bellows with shield.

is a computer code developed at KEK. ATF2 beamline optics is shown in Fig. 5.

We assumed that each wakefield source had a random misalignment and simulations were performed with 100 different random seeds. Based on the measurements, the misalignment of cavity BPM was set with 0.3 mm mean with 0.5 mm RMS, and other vacuum components were set with 0 mean and 1 mm RMS. The vacuum flange had the same misalignment with the attached wakefield source. The kick angle due to the wakefield, expressed as an angular change

MOP0TK043

557

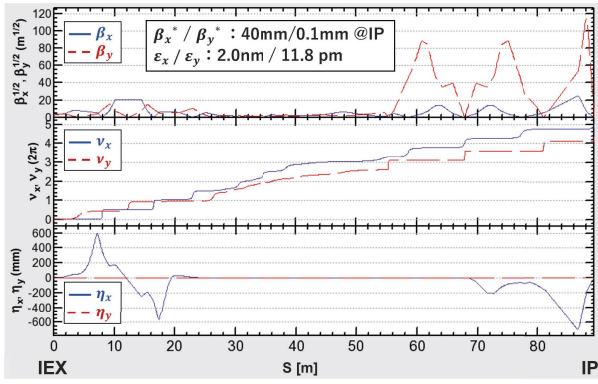


Figure 5: ATF2 design optics calculated by SAD.

Table 2: Calculation Results of Beam Size Growth by Wakefield (Bunch Population: 8.0e9).

	Wakefield Source	Misalign [mm]	Mean beamsize \pm SDOM [nm]
	No wake (design)		37.9
EXT	Septum magnet chamber*	± 1	37.8 ± 0.1
	Vacuum port*	± 1	37.9 ± 0.2
	Bellows	± 1	38.4 ± 0.7
EXT All			38.4 ± 0.7
FF	Cavity BPM	0.3 ± 0.5	40.8 ± 3.2
	Shielded vacuum port*	± 1	37.8 ± 0.007
	Shielded bellows*	± 1	40.9 ± 1.7
	Vacuum flange	-	43.8 ± 2.3
FF All			57.8 ± 3.3
EXT+FF All			66.4 ± 3.2

*newly calculated

$\Delta y'_{\text{wake}}$ of the particle, is:

$$\Delta y'_{\text{wake}} = \Delta p_y / p_0 = \frac{q_1}{E} W_y(x=0, y=\bar{y} - y_m, s_w) \quad (4)$$

$$\Delta y'_{\text{wake}} \approx \frac{q_1}{E} \sum_{i=0}^3 W_{yi}(x=0, s_w) (\bar{y} - y_m)^i, \quad (5)$$

where \bar{y} is the position of the center of the bunch, y_m is the misalignment of the wakefield source. We assumed offset dependence of the wakefield with scaling $q_1 W(y=1, s_w)y/E$ in the previous study. In this study, we took an offset dependence with 3rd order polynomial interpolation as Eq. 5 shown in Fig. 4 (dashed line).

Table 2 and Fig. 6 show the results. We evaluate effects of wakefield with the mean and standard deviation of the mean (SDOM) of the RMS beam size. Dashed lines are fitting curves, where ω and σ_{y0} are fitting parameters, Q is a beam intensity, and ω is an intensity dependence parameter that quantifies the effect of the wakefield. Table 2 shows beam size growth with the wakefield which is using scaled from the wakefield for 1mm offset. The effect of wakefield at the EXT beamline is smaller than the FF beamline because beta function in EXT beamline is much smaller. We compared results by major wakefield sources (cavity BPM,

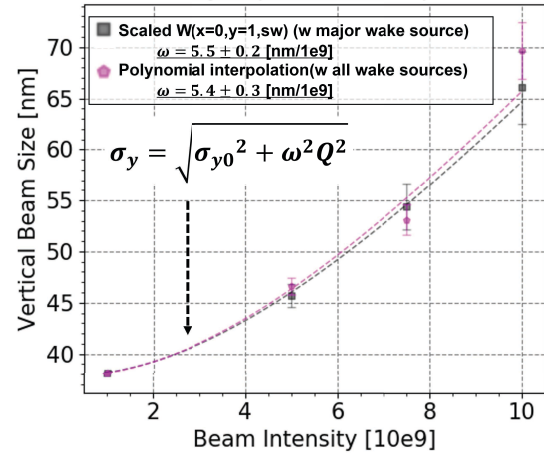


Figure 6: ATF2 intensity dependence calculation comparison. Vertical: IP beamsize, Horizontal: beam intensity.

bellows and vacuum flange) and by more realistically calculated wakefields (Table 2 *), and offset dependence of the wakefields with polynomial interpolation and bellows deformation (square and pentagon in Fig. 6). The deformation is derived as the difference of the misalignments of the bellows and its attached component.

As a result, there is no significant difference between two results. Effects of the newly considered wakefield are small even considering offset dependence and deformation. The result is similar to that in the previous study.

CONCLUSION

The intensity dependence of the beam size at ATF, mainly due to wakefield, were measured and simulated in the previous studies. We suspected some non-negligible wakefield sources existed because the experimental results were twice as large as the simulation results. We only considered major wakefield sources in the simulation with scaled wakefield to approximate offset dependence. Therefore, we have been performing more realistic simulation in order to understand the detail effects of the wakefield. The simulation includes wakefield sources, which were not considered in the past studies, and offset dependence with polynomial interpolation including bellows deformation.

The results are similar to that in the previous study. We have not considered the dynamic effects of orbit changes and realistic beam optics (e.g. magnet misalignment, x - y coupling and orbit feed back). We will continue the studies in order to understand the phenomena in the experiments clearly.

ACKNOWLEDGEMENTS

This work was supported by JST, the establishment of university fellowships towards the creation of science technology innovation, Grant Number JPMJFS2136. This work was also supported by JST SPRING, Grant Number SDP221102.

REFERENCES

- [1] “The International Linear Collider: Technical Design Report (TDR)”, Tech. Rep. ILC-REPORT-2013-040, 2013.
doi:10.48550/ARXIV.1306.6329
- [2] A. Aryshev *et al.*, “ATF report 2020”, Rev. Rep. CERN-ACC-2020-0029, CERN, Geneva, 2020.
- [3] J. Snuverink *et al.*, “Measurements and simulations of wakefields at the Accelerator Test Facility 2”, in *Phys. Rev. Accel. Beams*, vol. 19, p. 091002, 2016.
doi:10.1103/PhysRevAccelBeams.19.091002
- [4] P. Korysko, P. N. Burrows, A. Latina, and F. G. Angeles, “Wakefield effects and mitigation techniques for nanobeam production at the KEK Accelerator Test Facility 2”, *Phys. Rev. Accel. Beams*, vol. 23, p. 121004, 2020.
doi:10.1103/PhysRevAccelBeams.23.121004
- [5] T. Okugi, ATF International Collaboration, “Intensity dependence of ATF2 virtual IP beam size”, in *16th Annual Meeting of Particle Accelerator Society of Japan*, Kyoto, Japan, Oct. 2019, paper FRPI023.
- [6] GdfidL: <http://www.gdfidl.de/>
- [7] SAD: <http://acc-physics.kek.jp/SAD/>
- [8] K. Kubo, “ILC new luminosity design and small beam experiments at ATF”, presented at *Asian Linear Collider Workshop (ALCW'18)*, Fukuoka, Japan, 2018.